

Article

Adsorption of Ni(II) from Aqueous Media on Biodegradable Natural Polymers—Sarkanda Grass Lignin

Elena Ungureanu ¹, Costel Samuil ¹, Denis C. Țopa ¹, Ovidiu C. Ungureanu ², Bogdan-Marian Tofanică ³, Maria E. Fortună ^{4,*} and Carmen O. Brezuleanu ^{1,*}

¹ “Ion Ionescu de la Brad” Iasi University of Life Sciences, 3 Mihail Sadoveanu Alley, 700490 Iasi, Romania; elena.ungureanu@iuls.ro (E.U.); costel.samuil@iuls.ro (C.S.); denis.topa@iuls.ro (D.C.Ț.)

² “Vasile Goldis” Western University of Arad, 94 the Boulevard of the Revolution, 310025 Arad, Romania; ungureanu.ovidiu@uvvg.ro

³ “Gheorghe Asachi” Technical University of Iasi, 73 Prof. Dr. Docent Dimitrie Mangeron Blv., 700050 Iasi, Romania; b.m.tofanica@gmail.com

⁴ “Petru Poni” Institute of Macromolecular Chemistry, 41A Grigore Ghica Voda Alley, 700487 Iasi, Romania

* Correspondence: fortuna.maria@icmpp.ro (M.E.F.); olguta.brezuleanu@iuls.ro (C.O.B.)

Abstract: Heavy metals are pollutants that pose a risk to living systems due to their high toxicity and ability to accumulate and contaminate. This study proposes an alternative approach to the static adsorption of Ni(II) from aqueous media using Sarkanda grass lignin crystals, the non-cellulosic aromatic component of biomass, as an adsorbent substrate. To determine the best experimental conditions, we conducted tests on several parameters, including the initial and adsorbent solution pH, the concentration of Ni(II) in the aqueous solution, the amount of adsorbent used, and the contact time at the interface. The lignin’s adsorption capacity was evaluated using the Freundlich and Langmuir models to establish equilibrium conditions. The Lagergren I and Ho–McKay II kinetic models were used to determine the adsorption mechanism based on surface analyses and biological parameters such as the number of germinated seeds, energy, and germination capacity in wheat caryopses (variety *Glosa*) incorporated in the contaminated lignin and in the filtrates resulting from phase separation. The results suggest that Sarkanda grass lignin is effective in adsorbing Ni(II) from aqueous media, particularly in terms of adsorbent/adsorbate dosage and interfacial contact time.

Keywords: adsorption; Ni(II) ions; Sarkanda grass lignin; pollution; germination



Citation: Ungureanu, E.; Samuil, C.; Țopa, D.C.; Ungureanu, O.C.; Tofanică, B.-M.; Fortună, M.E.; Brezuleanu, C.O. Adsorption of Ni(II) from Aqueous Media on Biodegradable Natural Polymers—Sarkanda Grass Lignin. *Crystals* **2024**, *14*, 381. <https://doi.org/10.3390/cryst14040381>

Academic Editor: Pedro De Almeida

Received: 27 March 2024

Revised: 11 April 2024

Accepted: 16 April 2024

Published: 18 April 2024



Copyright: © 2024 by the authors. Licensee MDPI, Basel, Switzerland. This article is an open access article distributed under the terms and conditions of the Creative Commons Attribution (CC BY) license (<https://creativecommons.org/licenses/by/4.0/>).

1. Introduction

Although the negative impact of metal ions, such as Ni(II), Co(II), Cu(II), or Zn(II), on quality of life is well known, they are still widely used in many technological processes [1]. As a result, these ions are present in significant concentrations in aqueous effluents that are discharged into the environment, leading to long-term pollution [2]. The detection and analysis of such pollutants is crucial since heavy metals cannot be destroyed or degraded and tend to accumulate over time [3,4].

The elevated levels of nickel in nature have led to human pollution. This is evident in various sources such as glass, ceramic, and textile dyes, nickel-plated faucets, nickel–steel alloy tableware, and cigarette smoke [5]. Plants can act as biosorbents for heavy metals, including nickel, by absorbing them from the soil or through their aerial parts. While nickel is essential for plant metabolism, high concentrations can be dangerous for most plants [6–9]. Nickel has serious toxic potential in its gaseous form, nickel tetracarbonyl, which is considered responsible for the slow development of malignant formations [10]. Additionally, insoluble nickel oxide powders and soluble sulfate, nitrate, and chloride aerosols are also considered potential carcinogens [11–13]. To reduce pollution, it is necessary to not only decrease the amount of pollutants in the air, water, and soil but also explore options for recovering waste from industrial activities. The literature suggests various alternatives,

including the use of low-cost materials such as cellulosic and lignin biomass fractions for different purposes, as adsorbent materials for the retention of pollutant species [14–20], in gasification processes; as precursors in organic syntheses [21]; or as bio-cycle substances for the preservation of natural composite structures [22].

Lignin is a macromolecular compound with an aromatic structure and is the main component of biomass. It is produced worldwide in large quantities as a by-product/residue from pulp manufacturing or biomass hydrolysis technologies. Its potential for valorization is a real challenge at present [23], considering its origin from renewable resources, non-toxicity, and economic benefits due to its relatively low cost [24]. Lignin's porous and branched structure, high functional group content, and small, uniformly distributed active centers on its surface enable it to complex with polluting species, such as heavy metal ions, through ionic exchange. This facilitates the formation of stable donor–acceptor and ligno-complex bonds [25,26]. As a result, different types of lignins have been tested as substrates for heavy metal ion adsorption [15,18–21,27].

Adsorption processes are evaluated by obtaining adsorption isotherms, which are then interpreted using mathematical models. The most commonly used models are Freundlich and Langmuir [28,29]. These models indicate the mass of the solute retained by a given adsorbent under specific experimental conditions, such as the initial pH of the aqueous solution, sorbent dosage, initial concentration of the metal ion, and contact time between the two phases [20,30]. Studies on the kinetics of the adsorption process provide information on its mechanism [2,21]. However, the adsorption kinetics depend on both the adsorption process and the solute diffusion from the solution to the active centers on the adsorbent surface, and the level of relative humidity [31]. The two most commonly used kinetic models for approximating the mechanism of pollutant adsorption from aqueous solutions are the first-order Lagergren kinetic model and the second-order Ho–McKay kinetic model [20,32,33].

In this study, we evaluate the adsorption of Ni(II) from aqueous media under static conditions using Sarkanda grass lignin as the adsorption substrate. The evaluation is based on thermodynamic, kinetic, and biological parameters. Sarkanda grass lignin is a renewable, cheap, and non-toxic resource that shows promise as a future biosorbent, as supported by the experimental data obtained.

2. Materials and Methods

2.1. Materials

Main chemical materials: Unmodified Sarkanda grass lignin supplied by Granit Recherche Development S.A., Lausanne, Switzerland [20], and NiSO₄·6H₂O supplied by ChimReactiv S.R.L., Bucharest, Romania.

Biological material: Autumn wheat seeds (*Glosa*), a variety resistant to drought, overwintering, shattering, and current varieties of yellow rust, recommended for cultivation in southeastern Romania [34], offered by “Ion Ionescu de la Brad”, Iasi University of Life Sciences, Iasi, Romania. The seeds used in the experiments were harvested in 2023. The gluten content was 23.2%, protein content was 12.8%, lipid content was 1.14%, the hectoliter mass was 76 kg, and the mass of 1000 grains (MMB) was 41.8 g.

2.2. Experimental Procedure

2.2.1. Adsorption Experiments

To determine the optimal conditions for adsorption efficiency, we conducted preliminary experimental tests on initial Ni(II) concentrations, initial solution pH, adsorbent dosages, and contact times between the two phases. We chose to use 5 g of lignin per liter of the Ni(II) aqueous solution to ensure an adequate number of adsorption centers, considering the limited number of active centers in the lignin structure [20].

The carboxyl and hydroxyl functional groups on the lignin surface can deprotonate and associate via a Ni²⁺ donor–acceptor bond in the aqueous solution, re-emerging as ligno-complexes. Following experimental trials, a pH value of 5 was chosen, with

a moderate/low acid medium proving to be suitable in other systems, such as lignin–Pb(II)/Zn(II)/As(III)/Cd(II) [18–20].

Metal ion stock solutions were prepared by dissolving NiSO₄·6H₂O in distilled water to a concentration of 0.001 mg/L. Working solutions were then created by diluting a precisely measured volume of the stock solutions with distilled water. The concentrations of the metal ions in the resulting aqueous solutions are as follows: 5.8693, 11.738, 17.6079, 23.4772, 29.3465, 35.2158, 41.0851, 46.9544, 52.8237, and 58.693 mg/mL. A 20 mL volume of NiSO₄·6H₂O, with the concentrations mentioned above, was added to the lignin powder. The samples were then left to stand under laboratory conditions for different contact times (30, 60, and 90 min) to reach a steady state. This allowed for the optimal retention time of Ni²⁺ to be captured and for the kinetics of the process to be interpreted.

2.2.2. Germination Experiments

The effectiveness of lignin in adsorbing Ni(II) was also tested in a laboratory setting by evaluating the germination capacity of *Glosa* wheat seeds in three replicates, both on contaminated lignin and on filtrates. The biological process, expressed by germination energy and germination capacity, was monitored for 7 days. Distilled water was used as a control sample for filtrates, and an uncontaminated adsorbent was used for contaminated lignin.

2.3. Characterization Methods

2.3.1. Spectrophotometric Determination of Ni(II)

For determining the concentration of Ni(II), rubeanic acid was used, with maximum absorption at 590 nm. The rubeanic acid solution was obtained by dissolving 0.05 g of a solid reagent in 100 mL of 96% ethanol [1].

The quantitative determination of the metal ion obtained after filtration from the aqueous solutions was carried out by an analysis of an exactly measured volume (2 mL) according to the experimental procedure, and the concentration value for each sample was calculated from the regression equation of the calibration curve.

For the spectrophotometric analysis, we used a Visible Spectrophotometer for a laboratory, model VS-721N, 300–1000 nm, manufacturer JKI, Shanghai, China.

2.3.2. Isotherm Models

Adsorption isotherms characterize the interaction between the adsorbent and the adsorbate. They are interpreted using mathematical models, such as Freundlich or Langmuir, which are commonly used [35].

The adsorption capacities were determined according to the following equation [36]:

$$q = (c_i - c_e)V/m, \text{ (mg/g)} \quad (1)$$

where c_i is the initial concentration (mg/mL), c_e is the equilibrium concentration (mg/L), V is the volume of the metal ion solution (L), m is the mass of the adsorbent (g).

The Langmuir–Freundlich isotherm includes the knowledge of adsorption heterogeneous surfaces, such as the lignin surface. It describes the distribution of adsorption energy onto the heterogeneous surface of the adsorbent [37].

The Langmuir equation can be written in the following linear form [38]:

$$c_e/q_e = 1/q_m \cdot k_L + c_e/q_m \quad (2)$$

where q_e is the amount of metal ions adsorbed per unit of mass of the adsorbent (mg/g) at equilibrium, q_m is the maximum amount of metal ions retained on the adsorbent after saturation (mg/g), K_L is the Langmuir constant (L/mg), c_e is the equilibrium concentration of metal ions in the solution (mg/L).

The linear form of the Freundlich isotherm is as follows [39]:

$$\log q_e = \log k_F + 1/n \cdot \log c_e \quad (3)$$

where q_e is the amount of metal ions adsorbed per unit of mass of the adsorbent (mg/g) at equilibrium, K_F is the Freundlich constant (L/mg), n is the constant characterizing the affinity of metal ions to the adsorbent, c_e is the concentration at equilibrium of metal ions in the solution (mg/L).

The model that best reproduces the experimental isotherm data is selected based on the correlation coefficient R^2 values calculated using the method of least squares [35].

2.3.3. Kinetics Modeling

By kinetic modeling, the solute uptake rate is described, which in turn controls the residence time of sorbate uptake at the solid–solution interface [40]. For this purpose, the first-order Lagergren model and the second-order Ho–McKay model are frequently used, which can be applied to many different systems with different underlying mechanisms [41].

The Lagergren model is a mathematical representation of liquid–solid adsorption [42]:

$$\ln [q_e/(q_e - q)] = k_1 \cdot t \quad (4)$$

Most of the kinetic adsorption can be modeled well by the Ho–McKay model, thus indicating its superiority over other models [42]. Mathematically, it is expressed through the following relationship [41]:

$$t/q_t = (1/k_2 \cdot q_e^2) + t/q_e \quad (5)$$

where k_1 and k_2 are constant adsorption rates for model 1 and 2; q_e and q_t represent the adsorption capacity at equilibrium and at time t , respectively.

The experimental results were verified using the most suitable kinetic model chosen through linear regression.

2.3.4. Biological Stability

Germination tests were conducted on three batches of 20 wheat seeds (variety *Glosa*) under laboratory conditions with a temperature of $24 \text{ }^\circ\text{C} \pm 1$ and an illumination regime of 16 h light/8 h dark. Prior to testing, the seeds were disinfected with 5% sodium hypochlorite for 5 min and washed three times with MilliQ ultrapure water until the characteristic odor disappeared [43]. Wheat kernels were soaked in a filtrate or distilled water for one hour in $180 \times 18 \text{ mm}$ test tubes with intermittent shaking. The soaked seeds were then evenly distributed in $90 \times 15 \text{ cm}$ Petri dishes, each with two rounds of overlapping filter paper [20]. The toxicity of the filtrates and lignin contaminated with aqueous nickel solutions was analyzed at concentrations ranging from 5.8693 to 58.693 mg/mL and at three different contact times between phases. By using formulae (6) and (7), the germination energy and germination faculty can be determined within 30, 60, and 90 min [20,34]:

$$E_g = (a/n) \cdot 100 \quad (6)$$

$$F_g = (b/n) \cdot 100 \quad (7)$$

where a is the number of seeds germinated after three days, n is the total number of seeds analyzed, b is the number of seeds germinated at the end of the period (seven days).

Distilled water was used as a control sample for filtrates and uninfected lignin was used for contaminated lignin. It is worth mentioning that swollen, rotten, or moldy seeds at the end of the germination period were considered non-germinated.

2.3.5. Surface Morphology

Scanning electron microscopy (SEM) can be considered an efficient analysis method for organic and inorganic materials on the nanometer to micrometer (μm) scale. Energy dispersive radiography spectroscopy (EDS) provides fundamental qualitative and semi-quantitative results on the material and the species in its composition, which cannot be provided by common laboratory tests [44].

The SEM analysis was performed using the Quanta 200 scanning electron microscope (5 kV) equipped with an EDX elemental analysis system (Ametek, Berwyn, PA, USA). Quanta 200 SEM is a high-resolution environmental microscope (ESEM) capable of operating in high vacuum, variable pressure, and environmental modes. The specimens used were uncoated and untreated. The X-ray spectrometer was also utilized for element detection and spectral imaging.

3. Results and Discussion

3.1. Evaluation of Ni(II) Adsorption Efficiency on Sarkanda Grass Lignin through Analysis of Experimental Parameters Analyzed

3.1.1. Lignin Dose

The amount of adsorbent used affects adsorption and can provide valuable insights into the adsorption capacity of a material. This is primarily due to the availability of binding sites for removing a pollutant species at a specific concentration [16]. Preliminary tests were conducted to determine the optimal experimental conditions. The range of 4–40 g lignin/L Ni(II) aqueous solution, as proposed by study [21], was used. The results indicate that the ideal dose of lignin in Sarkanda grass should be 5 g/L Ni(II) aqueous solution, as seen in Figure 1.

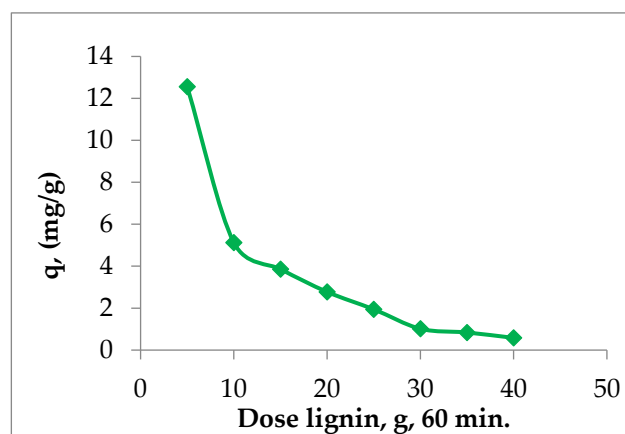


Figure 1. The influence of the Sarkanda grass lignin dose on the efficiency of the Ni(II) adsorption in a concentration of 58.693 mg/L, contact time of 60 min, pH of 5.

Figure 1 shows that increasing the lignin dose does not increase the adsorption rate, but instead decreases the amount of Ni(II) retained per unit mass of the adsorbent. This can be explained by the affinity between the functional groups on the surface of Sarkanda grass lignin and Ni(II), and possible complexation at adsorption initiation, after which the adsorbent pores become inaccessible. It is probable that saturation has been reached and that most of the functional groups in the lignin have been occupied, hindering the diffusion of Ni(II) to any unreacted (free) functional groups within the lignin.

3.1.2. Initial Concentration of Ni(II)

The concentration-dependent increase in Ni(II) resulted in a corresponding increase in the adsorption capacity of lignin. Specifically, the adsorption capacity increased from 1.2984 mg/g at a concentration of 5.86 mg/L to 12.5601 mg/g at a concentration of 58.69 mg/L after a contact time of 60 min (Figure 2). This increase can be attributed to the higher ratio between the initial number of Ni(II) moles and the number of accessible adsorption positions on the lignin fraction.

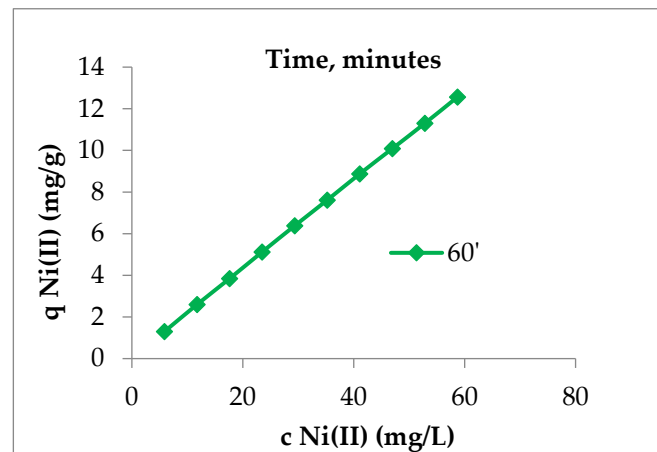


Figure 2. The adsorption capacity of the Sarkanda grass lignin, contact time of 60 min, pH of 5.

3.1.3. Contact Time

According to the literature, it is recommended that the contact time between phases be extended to capture crucial information about interfacial dynamics and the equilibrium [15]. The experimental data demonstrate that an increase in the contact time between the Sarkanda grass lignin and aqueous nickel solution results in a greater amount of the retained methyl-alkyl ion. This effect is more pronounced in the initial stage, after which the process slows down. The maximum amount is reached at 60 min, which can be considered the optimal time for achieving equilibrium (Figure 3). The 90 min contact time was excluded as there were no significant differences in adsorption capacity compared to the values recorded at 60 min.

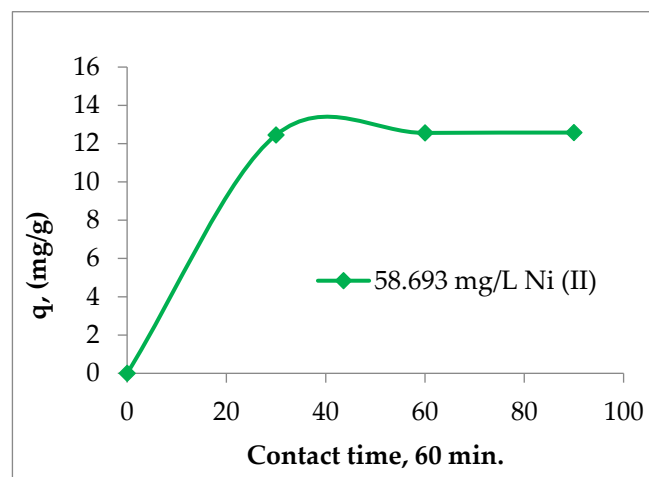


Figure 3. The influence of contact time on the adsorption of initial Ni(II) concentrations' solution on Sarkanda grass lignin.

3.1.4. pH Initial Solution

Figure 4 shows that the degree of lignin adsorption for Ni(II) increases as the initial pH of the solution increases. This is likely due to the deprotonation of functional groups on the lignin surface, which acquire a negative charge and can bind Ni(II) from the aqueous medium.

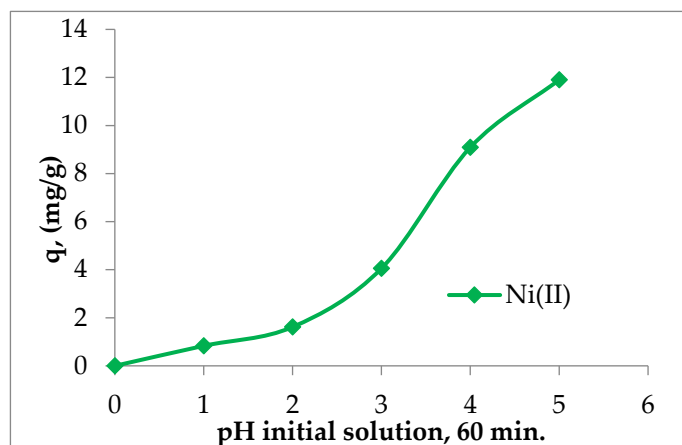


Figure 4. The influence of the pH of the initial solution on Ni(II) adsorption on Sarkanda grass lignin.

It is not recommended to use strongly acidic environments as the excess of protons can compete with nickel ions for the binding sites on lignin. Similarly, in alkaline environments, there is a possibility of the precipitation of Ni(II) in the form of an hydroxide, which reduces the efficiency of adsorption [2]. Based on the preliminary tests conducted on the adsorption of Ni(II) on Sarkanda grass lignin, it is recommended to use an optimal pH of 5. This is because the highest adsorption capacity values were obtained at this pH level.

3.2. Ni(II) Adsorption Efficiency on Sarkanda Grass Lignin Evaluated by Adsorption Isotherms

The adsorption isotherms obtained from the experiment provide valuable information about the interaction between the phases involved in adsorption [35]. These isotherms can be interpreted using mathematical models such as the Freundlich model, which can estimate adsorption on heterogeneous surfaces in a single or multiple layers, and the Langmuir model, which can describe retention in a single layer on a homogeneous surface [36].

The correlation coefficients (R^2) were calculated from the regression equations resulting from the linear representation of each individual model. Based on these coefficients, the most appropriate model can be chosen to describe the adsorption. Figure 5a,b display the linear representation of the Freundlich and Langmuir models for Ni(II) adsorption from aqueous media on Sarkanda grass lignin under optimal experimental conditions (temperature: 24 ± 0.5 °C, contact time: 60 min, pH 5). Table 1 presents the characteristic parameters of the Freundlich (R^2 , $1/n$, k_F) and Langmuir (R^2 , q_m , K_L) models under the same working conditions.

The correlation coefficients (R^2) obtained for the Langmuir model range from 0.7766 to 0.9179, slightly lower than those obtained for the Freundlich model, which range from 0.9822 to 0.9942 (Table 1). This suggests that the Freundlich model better describes the Ni(II) adsorption process on Sarkanda grass lignin. It is important to note that all evaluations are objective and based solely on the experimental data.

According to the literature, the Freundlich model is recommended for adsorption on heterogeneous surfaces or those composed of functional groups with different affinities for a given metal ion [40]. The low values of K_L , 0.0794–0.0801, suggest that the surface of Sarkanda grass lignin is not perfectly homogeneous, and therefore Ni(II) retention is not in the monolayer. Furthermore, it is important to note that the intensity of interactions between Ni(II) in the aqueous medium and the functional groups of lignin increases with higher values of K_F and $1/n$, as stated in references [20,40].

The analysis of the data presented in Table 1 shows that the values of K_F are in the range 1.9776–2.1586, and those of $1/n$ are in the range of 0.9028–0.9994. This suggests the occurrence of binding energy by adsorption due to ion-exchange interactions or surface complexation. However, it is unclear whether physical or chemical adsorption predominates, requiring a kinetic approach.

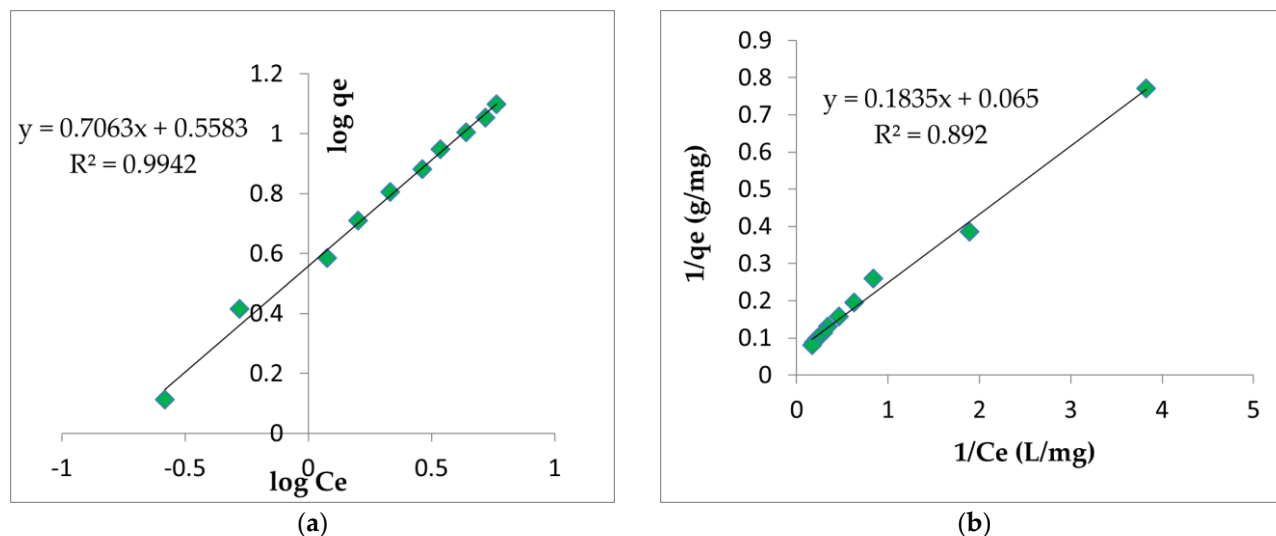


Figure 5. Freundlich adsorption model (a) and Langmuir adsorption model (b) for Ni(II) adsorption onto Sarkanda grass lignin after 60 min.

Table 1. Characteristic parameters of Freundlich and Langmuir models for Ni(II) adsorption on Sarkanda grass lignin.

Pollutant	Time (min)	Freundlich Model			Langmuir Model		
		R^2	$1/n$	k_F	R^2	q_m (mg/g)	K_L
Ni(II)	30	0.9822	0.9028	2.1586	0.9179	12.4073	0.0801
	60	0.9942	0.9205	2.0075	0.8920	12.5206	0.0795
	90	0.9844	0.9994	1.9776	0.7766	12.5398	0.0794

3.3. Efficiency Evaluation of Ni(II) Adsorption on Sarkanda Grass Lignin through Kinetic Modeling

To interpret the kinetics of Ni(II) adsorption on Sarkanda grass lignin, two mathematical models were employed: the pseudo-I-order Lagergren model, specific to liquid–solid adsorption, and the pseudo-II-order Ho and McKay model, which indicates the adsorption capacity of the solid phase. These models are known to accurately represent the adsorption processes according to study [45].

Figure 6a,b demonstrate the linear dependence for the Lagergren model of order I and the Ho–McKay model of order II for Ni(II) adsorption from aqueous media on Sarkanda grass lignin at an initial normalized concentration of 100 mg/mL. Table 2 presents the characteristic kinetic parameters calculated from the slopes and the intercept with the ordinate of the linear dependencies obtained for each kinetic model. The correlation coefficients (R^2) were obtained by linear regression.

The correlation coefficients (R^2) for the pseudo-I-order Lagergren kinetic model range from 0.6170 to 0.8731 (Table 2). These values are below 0.9, indicating the presence of electrostatic interactions between Ni(II) and the functional groups on the lignin surface. This suggests chemisorption rather than physical adsorption, which cannot be explained by the Lagergren model. Furthermore, the subunit values of R^2 restrict the applicability of this model for interpreting the kinetics of Ni(II) ion adsorption from aqueous media on Sarkanda grass lignin. This is consistent with previous research [18–20].

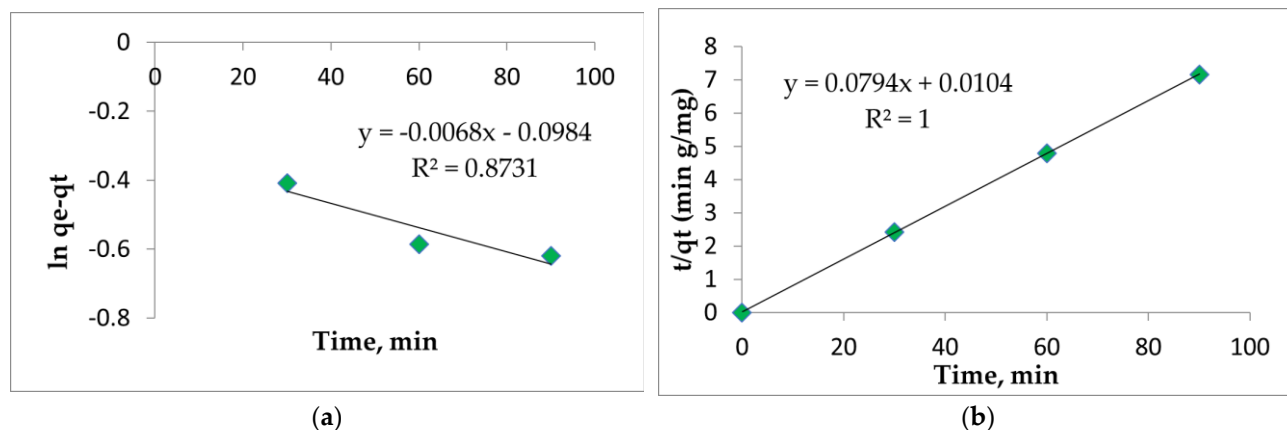


Figure 6. The linear representation of the Lagergren pseudo-I-order model (a) and Ho–McKay pseudo-II-order model (b) for the adsorption of Ni (II) onto Sarkanda grass lignin after 60 min.

Table 2. Kinetic parameters of the Lagergren and Ho–McKay models for Ni(II) adsorption on Sarkanda grass lignin.

Pollutant	c_i (mg/mL)	Lagergren Model			Ho–McKay Model		
		R^2	q_e (mg/g)	K_1 (min ⁻¹)	R^2	q_e (mg/g)	K_2 (g/mg·min)
Ni(II)	10	0.7903	1.1235	−0.0019	1	0.9421	1.2245
	20	0.7312	1.1643	−0.0016	1	5.5079	2.3469
	30	0.7759	4.1903	−0.0017	1	3.4399	4.1903
	40	0.6170	4.4132	−0.0021	1	6.1278	2.4210
	50	0.7052	5.4321	−0.0019	1	7.9889	2.9563
	60	0.8596	6.0234	−0.0017	1	8.8834	2.4369
	70	0.8477	7.2134	−0.0020	1	9.8973	1.8561
	80	0.7606	7.8321	−0.0020	1	10.0023	4.7597
	90	0.7697	8.0251	−0.0018	1	10.8250	2.8646
	100	0.8731	8.3267	−0.0019	1	10.6879	2.5011

After processing the experimental data using the pseudo-second-order Ho–McKay kinetic model, the correlation coefficients (R^2) showed a value of 1 in all cases (Table 2). The other parameters, q_e and K_2 , indicated a strong affinity of Ni(II) as a pollutant with Sarkanda grass lignin, which serves as a retention support. It is becoming more likely that the adsorption is active due to the presence of lignin’s functional groups, which can bond covalently and coordinatively with the metal ion to form a complex.

Ni(II) adsorption on Sarkanda grass lignin follows the Ho–McKay kinetic model of the pseudo II order. The rate-determining step of the adsorption process is the chemical interaction between the nickel ion in the aqueous medium and the functional groups of the biopolymer, particularly the carboxyl and hydroxyl groups.

3.4. Efficiency of Ni(II) Adsorption on Sarkanda Grass Lignin Evaluated through Biological Parameters

3.4.1. Number of Germinated Wheat Seeds, *Glosa* Variety

The presence of Ni(II) in the contaminated samples could cause the embryo of the wheat seeds to remain in a non-active or dormant state, disrupting osmotic equilibrium or metabolic functions. This results in an indirect toxic effect on the plants. Therefore, it is necessary to monitor the germination of the wheat caryopsis for seven days, as recommended in [34].

Figure 7a–c display the average number of germinated wheat seeds after three repetitions at 3 days for samples contaminated with Ni(II). The average number of germinated

seeds after three repetitions at 3 and 7 days for the filtrates resulting from the retention of Ni(II) at the three contact times between the phases is also shown.

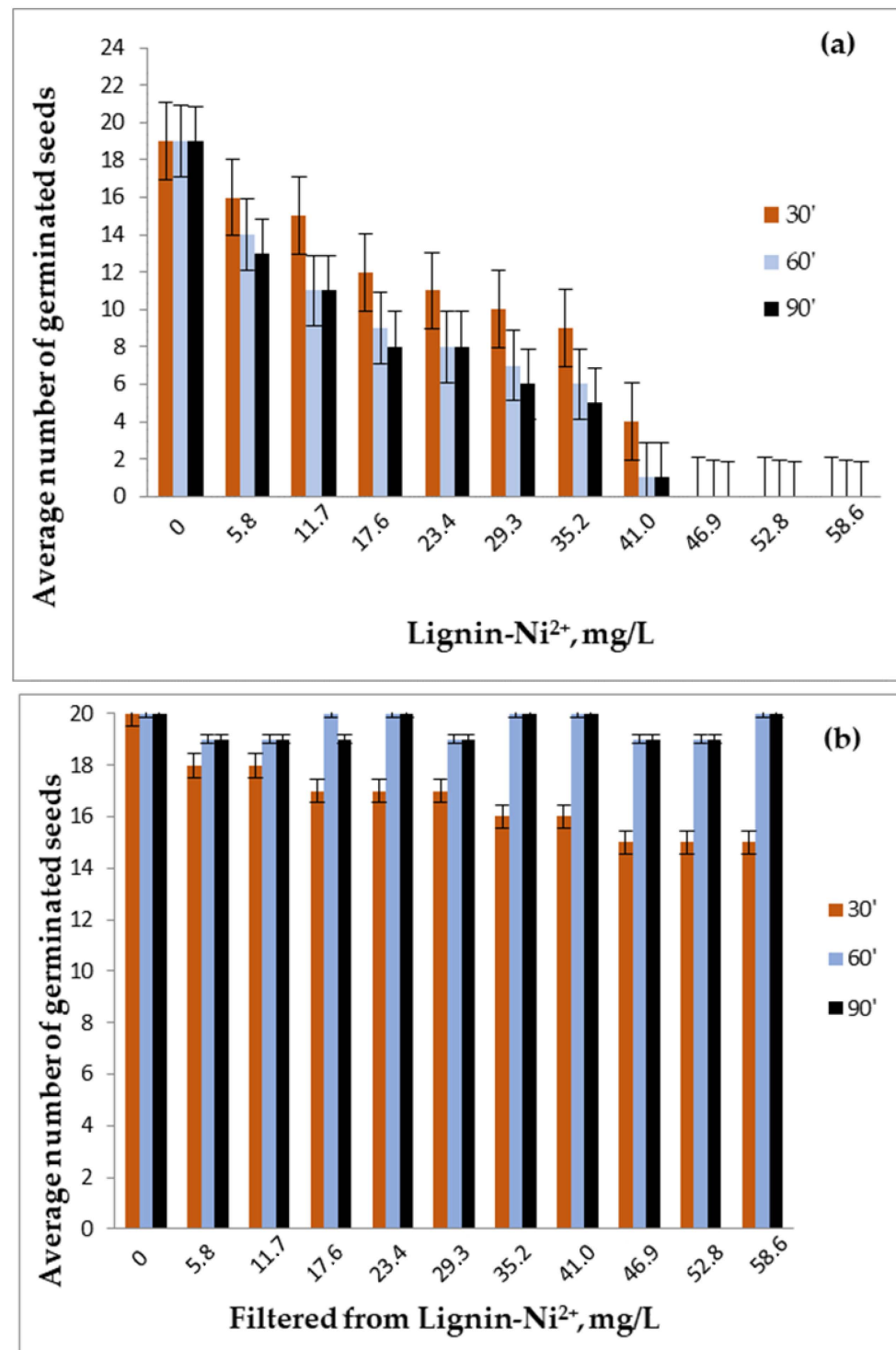


Figure 7. Cont.

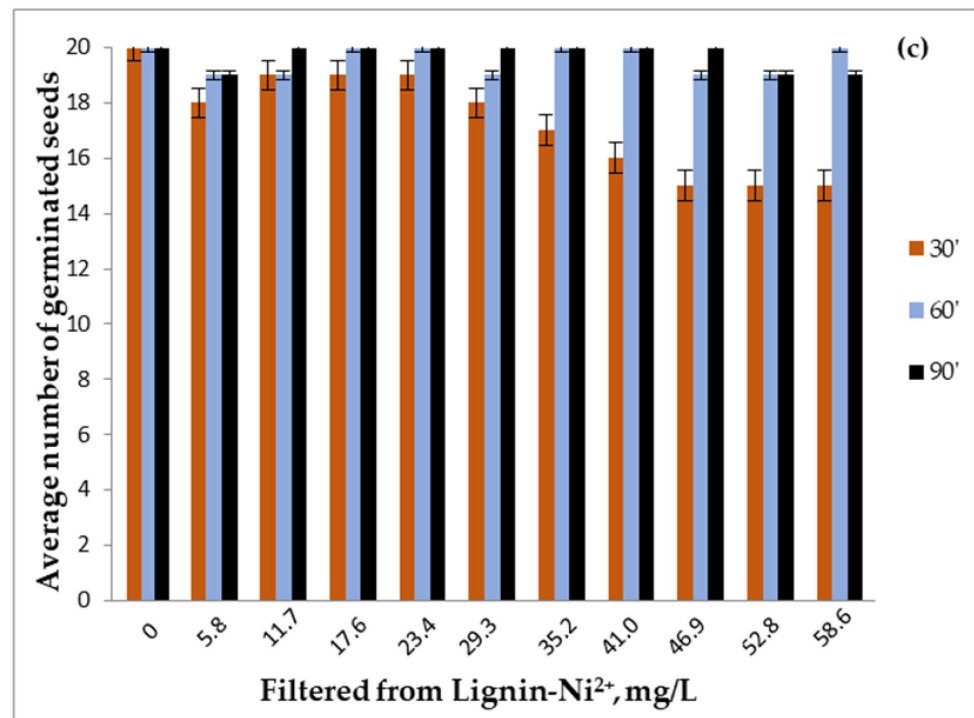


Figure 7. The average number of wheat seeds germinated at 3 days for the contaminated samples (a) and for the filtrates resulting from Ni(II) adsorption at 3 days (b) and 7 days (c).

From the analysis of Figure 7a–c, it is clear that Ni(II) has a negative effect on the germination of wheat caryopses, and this effect is enhanced by increasing the metal ion concentration and the duration of contact between the phases. In the control samples, 19 out of 20 seeds germinated in lignin and all 20 seeds germinated in distilled water. For the filtrates, the number of germinated seeds after 3 days and the number of seedlings after 7 days from germination are similar to those obtained in the control group at 60 and 90 min. However, at 30 min, the numbers are lower, indicating that the adsorption equilibrium is not reached within 30 min. Therefore, a longer contact time is required, which is consistent with the conclusions drawn from the interpretation of the adsorption isotherms and kinetic parameters. The optimal contact time is recommended to be 60 min.

At low Ni(II) concentrations and a contact time of 30 min, the highest number of germinated seeds appeared after 3 days when using contaminated lignin. Starting at a concentration of 35.2158 mg/L, less than half of the total 20 seeds germinated at all contact times. At a concentration of 46.9544 mg/L Ni(II), the seeds did not germinate, highlighting the toxic effect of nickel on seed germination with increasing concentration and duration of contact. Furthermore, after 7 days of germination, none of the contaminated lignin samples resulted in new germinated seeds or surviving seedlings, regardless of the contact times and Ni(II) concentration. This confirms the lignin's effective adsorption capacity for the pollutant species, as demonstrated by the obtained kinetic and chemical equilibrium results.

Figure 8 displays the germination of *Glosa* wheat seeds over seven days for four conditions: reference/uncontaminated lignin (R/UL), lignin contaminated with Ni(II) (CL), reference/distilled water (R/DW), and the filtrate (F) obtained after adsorption for 60 min at a concentration of 58.693 mg/L Ni(II).

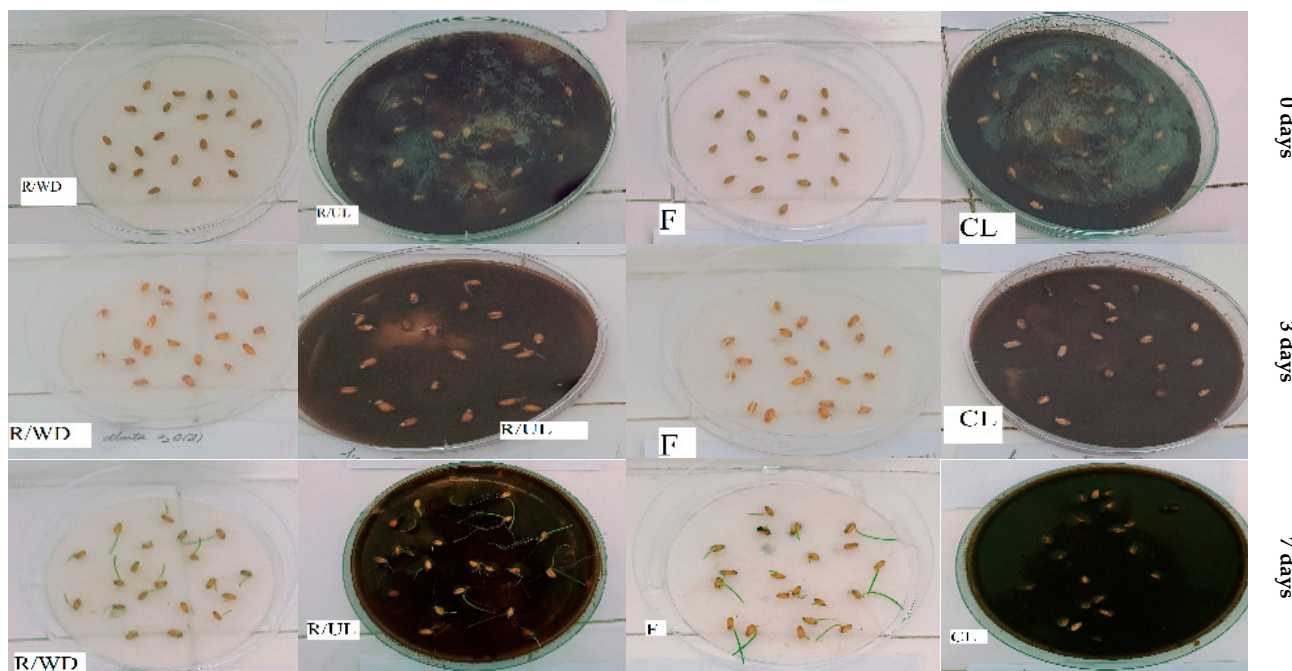


Figure 8. The germination of wheat seeds over a period of 7 days, at an adsorption time of 60 min and a concentration of 58.693 mg/L Ni (II).

3.4.2. Germination Energy and Capacity of Wheat Seeds, *Glosa* Variety

Table 3 shows that germination energy is correlated with the number of germinated seeds for both filtrates and samples of lignin contaminated with Ni(II). After 30 min of contact time between phases, there was no balance of adsorption. As a result, the filtrates were more concentrated, and the germination energy was lower. However, at 60 and 90 min, the germination energy was higher because the filtrates were more diluted due to the good retention capacity of lignin, eventually reaching saturation. In the concentration range of 46.9544–58.693 mg/L Ni²⁺, an increase in nickel concentration and contact time leads to a decrease in germination energy when contaminated with lignin. At all three contact times, the germination energy has zero values.

Table 3. The germination energy and capacity were measured for contaminated samples and filtrates resulting from Ni (II) retention at three different contact times between the phases. This was repeated three times to obtain an average.

Lignin/Ni(II) (mg/L)	Contact Time (Min)						Lignin/Ni(II) (mg/L) Filtered	Contact Time (Min)					
	30			60				30			60		
	Eg, %			Fg, %				Eg, %			Fg, %		
0	95	95	95	95	95	95	0	100	100	100	100	100	100
5.8693	80	70	65	0	0	0	5.8693	90	95	95	90	95	95
11.738	75	45	40	0	0	0	11.738	90	95	95	95	95	100
17.6079	60	40	40	0	0	0	17.6079	85	100	95	95	100	100
23.4772	55	35	30	0	0	0	23.4772	85	100	100	95	100	100
29.3465	50	30	25	0	0	0	29.3465	85	95	95	90	95	100
35.2158	45	10	10	0	0	0	35.2158	80	100	100	85	100	100
41.0851	20	0	0	0	0	0	41.0851	80	100	100	80	100	100
46.9544	0	0	0	0	0	0	46.9544	75	90	95	75	95	100
52.8237	0	0	0	0	0	0	52.8237	75	90	95	75	95	95
58.693	0	0	0	0	0	0	58.693	75	100	100	75	100	100

In regards to the germinative capacity, filtrates show a proportional variation with the germinative energy, whereas contaminated lignin consistently records zero values. Furthermore, the germination energy and capacity in the filtrate samples were similar to those in the control sample, regardless of the concentration of Ni(II). However, at contact times greater than 30 min, there were negligible differences at 60 and 90 min. This confirms the efficient adsorption of Ni(II) on Sarkanda grass lignin at a contact time of 60 min, which is considered optimal in terms of chemical and kinetic equilibrium results.

The biological tests show that Sarkanda grass lignin is efficient in retaining Ni(II) from an aqueous solution due to the good affinity of the species involved. The evaluation of parameters demonstrates this efficiency.

3.5. Efficiency of Ni(II) Adsorption on Sarkanda Grass Lignin Evaluated through Surface Analyses

In Figures 9 and 10, the morphology and composition of lignin before the adsorption and after the adsorption of Ni (II) at a concentration of 58.693 mg/L and a contact time of 60 min are presented, which were obtained by scanning electron microscopy (SEM) coupled with X-ray analysis Energy Dispersive X (EDX).

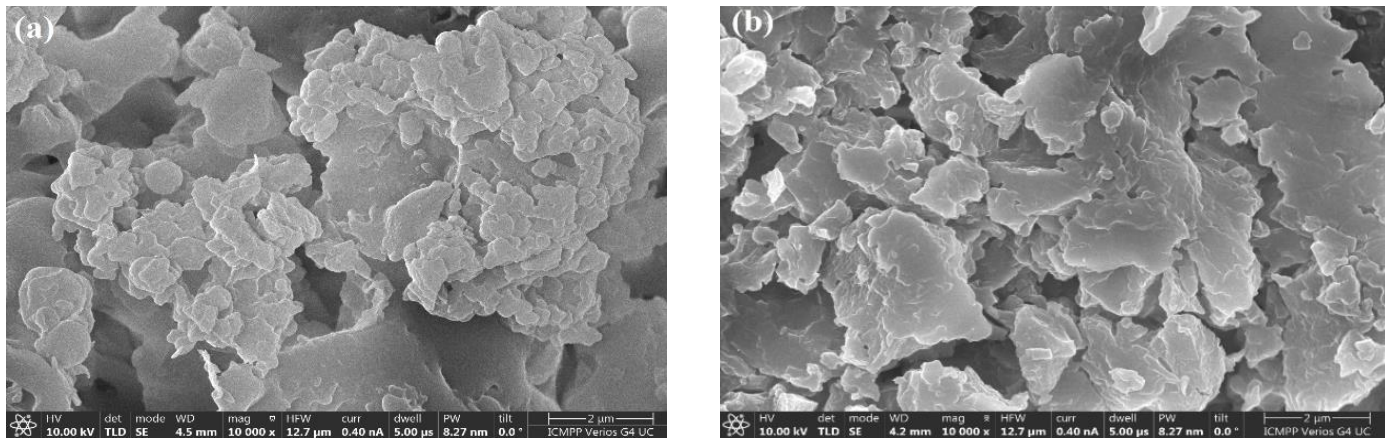


Figure 9. The SEM images for Sarkanda grass lignin before adsorption (a) and after Ni(II) adsorption (b).

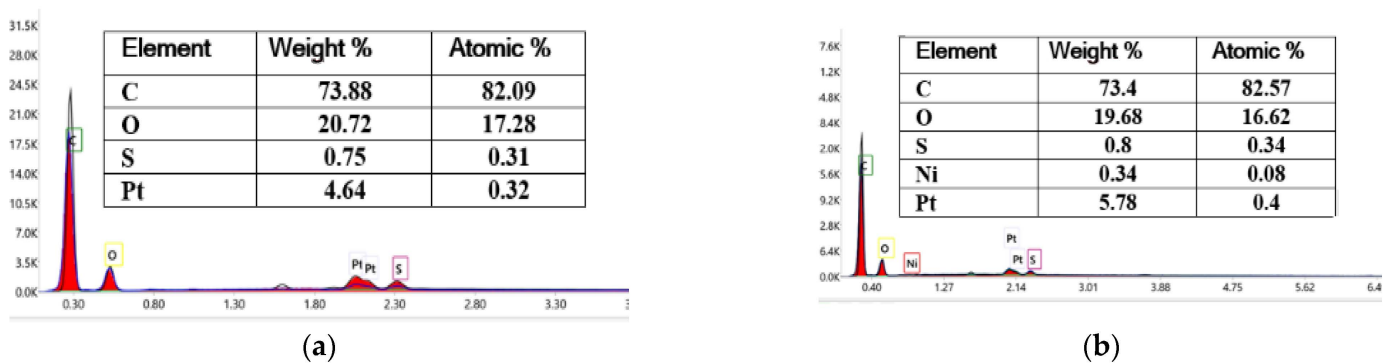


Figure 10. The EDX elemental analysis for lignin before adsorption (a) and after Ni(II) adsorption (b).

For the SEM analysis, the prepared sample has been metallized with Pt to improve the contrast, thus resulting in Pt in both samples. The SEM micrograph of the uncontaminated lignin clearly shows a well-separated particle agglomeration of approximately a 4 μm length (Figure 9a). The micrometric dimensions of these particles that form aggregates were also confirmed by the diffraction analyzer. It can be seen that the surface morphology of the unmodified lignin was different from the one observed for lignin contaminated with Ni(II), a fact that confirms the contact between the two phases, the

diffusion of the polluting species, and its adsorption in the pores of the lignin polymer (Figure 9b).

Sarkanda grass lignin composition before and after NiSO₄ adsorption was obtained using the EDX analysis. The EDX spectra for the samples are shown in Figure 10a,b, showing the main peaks of C, O, and S elements originating from both samples, and the EDX spectrum for lignin after Ni(II) adsorption clearly shows nickel adsorption.

In line with the trend toward sustainable development, bio-based adsorbents—which are abundant, inexpensive, and environmentally friendly—have emerged as potential sustainable alternatives to conventional synthetic adsorbents in the water purification industry. Lignocellulosic systems are highly structured and provide abundant adsorption sites for metal ion uptake thanks to various functional groups, such as hydroxyl (–OH), carboxyl (–COOH), and phenolic (–Ph) groups, that have the ability to form chemical bonds with them. For example [46,47], unmodified cellulose retains 32–40 mg/g of Cd²⁺, Zn²⁺, Ni²⁺, and Pb²⁺ at a contact time of 60 min and pH of 5–7. The same and different untreated agricultural wastes had a similar adsorption capacity of 7–56 mg/g in a similar condition. In earlier research [18–20], Sarkanda grass lignin was capable of retaining an average of 9 mg/g of Zn²⁺, up to 17 mg/g of Cd²⁺ and As³⁺, and up to 30 mg/g of Pb²⁺, which makes lignin a highly effective biosorbent.

Based on the reproducibility of observations in the surface analysis, kinetic data, chemical balance, and biological stability, this study recommends Sarkanda grass lignin as an effective adsorbent for polluting species, such as metal ions in aqueous environments. This recommendation is supported by the performance of the retention itself and the economic profitability resulting from the function of lignin as an easily renewable bio-resource and non-polluting waste.

4. Conclusions

Under precisely established experimental conditions, including a temperature of 24 ± 0.5 °C, moderate/weak acid pH of 5 for both lignin and Ni(II) aqueous solutions, a dose of 5 g adsorbent/L pollutant solution, and a concentration range of 46.9544–58.693 mg/L Ni²⁺, Sarkanda grass lignin has been identified as a potential adsorbent with high efficiency for retaining Ni(II) from aqueous media.

The correlation coefficients obtained from the Freundlich and Langmuir models were used to interpret the experimental adsorption isotherms and establish the efficiency of the adsorbent from a practical standpoint. However, they could not determine whether the adsorption was physical or chemical. The Freundlich model was found to be more appropriate for describing the retention of Ni(II) on the heterogeneous and porous surface of lignin, indicating a higher probability of chemisorption. This also proved the efficiency of the polymer as an adsorbent. Furthermore, SEM and EDX surface analyses clearly confirm the adsorption of Ni(II) in the pores of Sarkanda grass lignin.

Based on the interpretation of the kinetic data using the Lagergren model of the pseudo I order and Ho–McKay model of the pseudo II order, it appears that the Ho–McKay model is the most suitable for describing the adsorption of Ni(II) from aqueous media on Sarkanda grass lignin. This provides conclusive evidence regarding the electrostatic nature of the interactions between the two species involved and the triggering of an active chemical adsorption due to the good complexing capacity of lignin.

The biological analyses were conducted on *Glosa* wheat seeds incorporated in lignin contaminated with a Ni(II) aqueous solution at concentrations ranging from 46.9544 to 58.693 mg/L Ni²⁺. The filtrates resulting from the separation of the two phases after adsorption were also analyzed at three different contact times. The biopolymer has demonstrated good retention capacity at 30, 60, and 90 min. This is likely due to the abiotic stress caused by the inhibitory effect of Ni(II) on the biological dynamics associated with the germination of wheat caryopses and subsequent seedling development.

From the perspective of the obtained experimental parameters, Sarkanda grass lignin appears to be a viable alternative for adsorbing certain pollutants, such as heavy

metals, instead of Ni(II). This is due to the variety and large number of superficial functional groups present in the porous and heterogeneous structure of the polymer, which facilitates processes of ion exchange or complexation with metal ions. Additionally, it is available in large quantities globally, as it is a renewable waste resource, which can be economically profitable, and it is non-polluting.

Our future research efforts will focus on the potential of lignin as an adsorbent for heavy metal removal, exploring its effectiveness in adsorbing other heavy metals, both individually and in mixtures or combinations. This approach will allow us to assess the versatility and applicability of Sarkanda grass lignin in a wider range of environmental contexts and pollutant scenarios, contributing to the development of sustainable and environmentally friendly solutions for water purification and pollution mitigation.

Author Contributions: Conceptualization, E.U., M.E.F., and O.C.U.; methodology, C.O.B. and C.S.; investigation, E.U., M.E.F., and D.C.T.; resources, E.U., B.-M.T., and C.S.; writing—original draft preparation, M.E.F., E.U., and O.C.U.; writing—review and editing, E.U., B.-M.T., M.E.F., and D.C.T.; visualization, E.U., O.C.U., and M.E.F.; software, D.C.T. and B.-M.T.; supervision, C.S. and C.O.B. All authors have read and agreed to the published version of the manuscript.

Funding: This research received no external funding.

Data Availability Statement: The original contributions presented in the study are included in the article, further inquiries can be directed to the corresponding author.

Conflicts of Interest: The authors declare no conflicts of interest.

References

1. Fornea, V.; Trupină, S.; Iosub, A.V.; Bulgariu, L. Spectrophotometric determination of Cu(II), Co(II) and Ni(II) ions in mono and multi-component systems. *Bul. Inst. Polit.* **2016**, *62*, 11–20.
2. Pavel, L.V. Behavioral Studies of Heavy Metals in the Soil and of some Remedy Alternatives. Ph.D. Thesis, “Gh. Asachi” Polytechnic University of Iasi, Iasi, Romania, 2012; pp. 31–39.
3. Jaishankar, M.; Tseten, T.; Anbalagan, N.; Mathew, B.B.; Mathew, K.N. Toxicity, mechanism and health effects of some heavy metals. *Rev. Interdiscip. Toxicol.* **2014**, *7*, 60–72. [[CrossRef](#)] [[PubMed](#)]
4. Duruibe, J.O.; Ogwuegbu, M.O.C.; Egwurugwu, J.N. Heavy metal pollution and human biotoxic effects. *Phys. Sci. Int. J.* **2007**, *2*, 112–118.
5. Begum, W.; Rai, S.; Banerjee, S.; Bhattacharjee, S.; Mondal, M.H.; Bhattarai, A.; Saha, B. A comprehensive review on the sources, essentiality and toxicological profile of nickel. *RSC Adv.* **2022**, *12*, 9139–9153. [[CrossRef](#)] [[PubMed](#)]
6. Cavani, A. Breaking tolerance to nickel. *Toxicology* **2005**, *209*, 119–121. [[CrossRef](#)] [[PubMed](#)]
7. Rothenberg, S.J.; Karchmer, S.; Schnaas, L.; Perroni, E.; Zea, F.; Fernandez, A.J. Change in serial blood lead levels during pregnancy. *Environ. Health Perspect.* **1994**, *102*, 876–880. [[CrossRef](#)] [[PubMed](#)]
8. Pokorska-Niewiada, K.; Rajkowska-Myśliwiec, M.; Protasowicki, M. Acute lethal toxicity of heavy metals to the seeds of plants of high importance to humans. *Bull. Environ. Contam.* **2018**, *101*, 222–228. [[CrossRef](#)] [[PubMed](#)]
9. Khan, Z.I.; Ahmad, K.; Ahmad, T.; Zafar, A.; Alrefaei, A.F.; Ashfaq, A.; Akhtar, S.; Mahpara, S.; Mehmood, N.; Ugulu, I. Evaluation of nickel toxicity and potential health implications of agriculturally diversely irrigated wheat crop varieties. *Arab. J. Chem.* **2023**, *16*, 104934. [[CrossRef](#)]
10. Genchi, G.; Carocci, A.; Lauria, G.; Sinicropi, M.S.; Catalano, A. Nickel: Human Health and Environmental Toxicology. *Int. J. Environ. Res. Public Health* **2020**, *17*, 679. [[CrossRef](#)]
11. Shen, H.M.; Zhang, Q.F. Risk assessment of nickel carcinogenicity and occupational lung cancer. *Environ. Health Perspect.* **1994**, *102*, 275–282. [[CrossRef](#)]
12. Ellen, T.P.; Kluz, T.; Harder, M.E.; Xiong, J.; Costa, M. Heterochromatinization as a potential mechanism of nickel-induced carcinogenesis. *Biochemistry* **2009**, *48*, 4626–4632. [[CrossRef](#)] [[PubMed](#)]
13. Zou, L.; Su, L.; Sun, Y.; Han, A.; Chang, X.; Zhu, A.; Liu, F.; Li, J.; Sun, Y. Nickel sulfate induced apoptosis via activating ROS-dependent mitochondria and endoplasmic reticulum stress pathways in rat Leydig cells. *Environ. Toxicol.* **2017**, *32*, 1918–1926. [[CrossRef](#)] [[PubMed](#)]
14. Sciban, M.; Klasnja, M.; Skrbic, B. Modified softwood sawdust as adsorbent of heavy metal ions from water. *J. Hazard. Mater.* **2006**, *136*, 266–271. [[CrossRef](#)] [[PubMed](#)]
15. Guo, X.Y.; Zhang, A.Z.; Shan, X.Q. Adsorption of metal ions on lignin. *J. Hazard. Mater.* **2008**, *151*, 134–142. [[CrossRef](#)] [[PubMed](#)]
16. Zhang, Z.; Chen, Y.; Wang, D.; Yu, D.; Wu, C. Lignin-based adsorbents for heavy metals. *Ind. Crops Prod.* **2023**, *193*, 116119. [[CrossRef](#)]

17. Hubbe, M.A.; Beck, K.R.; O'Neal, W.G.; Sharma, Y.C. Cellulosic substrates for removal of pollutants from aqueous systems: A review. 2. Dyes. *BioResources* **2012**, *7*, 2592–2687. [[CrossRef](#)]
18. Ungureanu, E.; Trofin, A.; Trincă, L.C.; Ariton, A.M.; Ungureanu, O.C.; Fortună, M.E.; Jităreanu, C.D.; Popa, V.I. Studies on kinetics and adsorption equilibrium of lead and zinc ions from aqueous solutions on Sarkanda Grass lignin. *Cellul. Chem. Technol.* **2021**, *55*, 939–948. [[CrossRef](#)]
19. Ungureanu, E.; Jităreanu, C.D.; Trofin, A.; Fortună, M.E.; Ungureanu, O.C.; Ariton, A.M.; Trincă, L.C.; Brezuleanu, S.; Popa, V.I. Use of Sarkanda Grass lignin as a possible adsorbent for As (III) from aqueous solutions—kinetic and equilibrium studies. *Cellul. Chem. Technol.* **2022**, *56*, 681–689. [[CrossRef](#)]
20. Ungureanu, E.; Fortună, M.E.; Țopa, D.C.; Brezuleanu, C.O.; Ungureanu, V.I.; Chiruță, C.; Rotaru, R.; Tofanică, B.M.; Popa, V.I.; Jităreanu, D.C. Comparison adsorption of Cd (II) onto Lignin and Polysaccharide-based polymers. *Polymers* **2023**, *15*, 3794. [[CrossRef](#)]
21. Rusu, G. Studies on the Use of Cellulosic Wastes in Reducing Environmental Pollution. Ph.D. Thesis, “Gh. Asachi” Polytechnic University of Iasi, Iasi, Romania, 2015; pp. 29–48.
22. Ungureanu, E. Aspects of Composites Biodegradation Based on Lignocelluloses Materials. Ph.D. Thesis, “Gh. Asachi” Polytechnic University of Iasi, Iasi, Romania, 2008; pp. 15–20.
23. Sethupathy, S.; Morales, G.M.; Gao, L.; Wang, H.; Yang, B.; Jiang, J.; Sun, J.; Zhu, D. Lignin valorization: Status, challenges and opportunities. *Bioresour. Technol.* **2022**, *347*, 126696. [[CrossRef](#)]
24. Mabrouka, A.; Erdociab, X.; Alriolsb, M.G.; Labidib, J. Techno-Economic Evaluation for Feasibility of Lignin Valorisation Process for the Production of Bio-Based Chemicals. *Chem. Eng. Trans.* **2017**, *61*, 428–432.
25. Garcia-Valls, R.; Hatto, T.A. Metal ion complexation with lignin derivatives. *J. Chem. Eng.* **2003**, *94*, 99–105. [[CrossRef](#)]
26. Todorciuc, T. Contributions to Some Complex Combinations of Natural Products with Aromatic Structure. Ph.D. Thesis, “Gh. Asachi” Polytechnic University of Iasi, Iasi, Romania, 2016; pp. 62–78.
27. Wang, X.; Li, X.; Peng, L.; Han, S.; Hao, C.; Jiang, C.; Wang, H.; Fan, X. Effective removal of heavy metals from water using porous lignin-based adsorbents. *Chemosphere* **2021**, *279*, 130504. [[CrossRef](#)]
28. Weber, W.J.J.; McGinley, P.M.; Katz, L.E. Sorption phenomena in subsurface systems: Concepts, models and effects on contaminant fate and transport. *Water Res.* **1991**, *25*, 499–528. [[CrossRef](#)]
29. Chong, K.H.; Volesky, B. Description of two-metal biosorption equilibria by Langmuir-type models. *Biotechnol. Bioeng.* **1995**, *47*, 451–460. [[CrossRef](#)]
30. Rajeev, A. Adsorption of Heavy Metals—A Review. *Mater. Today Proc.* **2019**, *18*, 4745–4750.
31. Marcuello, C.; Foulon, L.; Chabbert, B.; Aguié-Béghin, V.; Molinari, M. Atomic force microscopy reveals how relative humidity impacts the Young's modulus of lignocellulosic polymers and their adhesion with cellulose nanocrystals at the nanoscale. *Int. J. Biol. Macromol.* **2020**, *147*, 1064–1075. [[CrossRef](#)] [[PubMed](#)]
32. Azizian, S. Kinetic models of sorption: A theoretical analysis. *J. Colloid Interface Sci.* **2004**, *276*, 47–52. [[CrossRef](#)]
33. Revellame, E.D.; Fortela, D.L.; Sharp, W.; Hernandez, R.; Zappi, M.E. Adsorption kinetic modeling using pseudo-first order and pseudo-second order rate laws: A review. *Clean. Eng. Technol.* **2020**, *1*, 100032. [[CrossRef](#)]
34. Samuil, C. *General Plant Technologies*; University of Agricultural Sciences and Veterinary Medicine Ion Ionescu de la Brad: Iasi, Romania, 2010; p. 280.
35. Ayawei, N.; Ebelegi, A.N.; Wankasi, D. Modelling and Interpretation of Adsorption Isotherms. *J. Chem.* **2017**, *2017*, 3039817. [[CrossRef](#)]
36. Hanif, M.A.; Tauqeer, H.M.; Aslam, N.; Hanif, A.; Yaseen, M.; Khera, R.A. Correct Interpretation of sorption mechanism by Isothermal, Kinetic and Thermodynamic models. *Int. J. Chem. Biochem. Sci.* **2017**, *12*, 53–67.
37. Koble, R.A.; Corrigan, T.E. Adsorption isotherms for pure hydrocarbons. *J. Ind. Eng. Chem.* **1952**, *44*, 383–387. [[CrossRef](#)]
38. Dabrowski, A. Adsorption—From theory to practice. *Adv. Colloid Interface Sci.* **2001**, *93*, 135–224. [[CrossRef](#)] [[PubMed](#)]
39. Boparai, H.K.; Joseph, M.; O'Carroll, D.M. Kinetics and thermodynamics of cadmium ion removal by adsorption onto nano zerovalent iron particles. *J. Hazard. Mater.* **2011**, *186*, 458–465. [[CrossRef](#)] [[PubMed](#)]
40. Ho, Y.S.; McKay, G. Pseudo-second order model for sorption processes. *Process Biochem.* **1999**, *34*, 451–465. [[CrossRef](#)]
41. Major, G.H.; Chatterjee, S.; Linford, M.R. Resolving a mathematical inconsistency in the Ho and McKay adsorption equation. *Appl. Surf. Sci.* **2020**, *504*, 144157. [[CrossRef](#)]
42. Tan, K.L.; Hameed, B.H. Insight into the Adsorption Kinetics Models for the Removal of Contaminants from Aqueous Solutions. *J. Taiwan Inst. Chem. Eng.* **2017**, *74*, 25–48.
43. Iyem, E.; Yildirim, M.; Kizilgeci, F. Germination, seedling growth and physio-biochemical indices of bread wheat (*Triticum aestivum* L.) genotypes under peg induced drought stress. *Agric. For.* **2021**, *67*, 163–180. [[CrossRef](#)]
44. Mohammed, A.; Abdullah, A. Scanning Electron Microscopy (SEM): A Review. In Proceedings of the 2018 International Conference on Hydraulics and Pneumatics—HERVEX, Băile Govora, Romania, 7–9 November 2018; Volume 1, pp. 77–85.
45. Aziam, R.; Chibana, M.; Eddaoudi, H.; Soudani, A.; Zerbet, M.; Sinan, F. Kinetic modeling, equilibrium isotherm and thermodynamic studies on a batch adsorption of anionic dye onto eco-friendly dried *Carpobrotus edulis* plant. *Eur. J. Phys.* **2017**, *226*, 977–992. [[CrossRef](#)]

46. Kainth, S.; Piyush Sharma, P.; Pandey, O.P. Green sorbents from agricultural wastes: A review of sustainable adsorption materials. *Appl. Surf. Sci. Adv.* **2024**, *19*, 100562–100583. [[CrossRef](#)]
47. Raji, Z.; Karim, A.; Karam, A.; Khalloufi, S. Adsorption of Heavy Metals: Mechanisms, Kinetics, and Applications of Various Adsorbents in Wastewater Remediation—A Review. *Waste* **2023**, *1*, 775–805. [[CrossRef](#)]

Disclaimer/Publisher’s Note: The statements, opinions and data contained in all publications are solely those of the individual author(s) and contributor(s) and not of MDPI and/or the editor(s). MDPI and/or the editor(s) disclaim responsibility for any injury to people or property resulting from any ideas, methods, instructions or products referred to in the content.